8s, a numerical simulator of the challenging optical calibration of the E-ELT adaptive mirror M4

Briguglio, Runa, Pariani, Giorgio, Xompero, Marco, Riccardi, Armando, Tintori, Matteo, et al.

Runa Briguglio, Giorgio Pariani, Marco Xompero, Armando Riccardi, Matteo Tintori, Paolo Lazzarini, Paolo Spanò, "8s, a numerical simulator of the challenging optical calibration of the E-ELT adaptive mirror M4," Proc. SPIE 9909, Adaptive Optics Systems V, 99097A (27 July 2016); doi: 10.1117/12.2231634

SPIE.

Event: SPIE Astronomical Telescopes + Instrumentation, 2016, Edinburgh, United Kingdom

8s, a numerical simulator of the challenging optical calibration of the E-ELT adaptive mirror M4

Runa Briguglio[a], Giorgio Pariani[b], Marco Xompero[a], Armando Riccardi[a], Matteo Tintori[c], Paolo Lazzarini[c], and Paolo Spanò[a]

[a]INAF Osservatorio Astrofisico Arcetri L. E. Fermi 5, 50125 Firenze Italy
[b]INAF Osservatorio Astronomico Brera, via E. Bianchi 46, 23807 Merate (LC) Italy
[c]ADS-International, via Roma 87, 23868 Valmadrera (LC) Italy

ABSTRACT

8s stands for Optical Test TOwer Simulator (with 8 read as in italian 'otto'): it is a simulation tool for the optical calibration of the E-ELT deformable mirror M4 on its test facility. It has been developed to identify possible criticalities in the procedure, evaluate the solutions and estimate the sensitivity to environmental noise. The simulation system is composed by the finite elements model of the tower, the analytic influence functions of the actuators, the ray tracing propagation of the laser beam through the optical surfaces. The tool delivers simulated phasemaps of M4, associated with the current system status: actuator commands, optics alignment and position, beam vignetting, bench temperature and vibrations. It is possible to simulate a single step of the optical test of M4 by changing the system parameters according to a calibration procedure and collect the associated phasemap for performance evaluation. In this paper we will describe the simulation package and outline the proposed calibration procedure of M4.

Keywords: Adaptive Optics, Wavefront correctors, Deformable mirrors, Optical calibration, Simulation

1. OPTICAL CALIBRATION OF M4, THE E-ELT DEFORMABLE MIRROR

The adaptive M4 Unit (M4U), the ground-layer wavefront corrector of the E-ELT, will be the largest deformable mirror equipping an astronomical AO system. M4U is a 2.4m flat deformable mirror, segmented into six petals, shaped by 5316 voice-coil actuators. It is now under the Final Design Phase by AdOptica, the Consortium of the two Italian Companies Microgate and A.D.S. International, along with the scientific partnership of INAF and Politecnico di Milano. M4U is hold by a hexapod providing tip-tilt and decentering, while a focus selector switches between the two Nasmyth foci of the telescope. M4U will provide shaping and fast steering capabilities for the real-time atmospheric turbulence and wind shaking correction in addition to static aberrations compensation.[1] The the first light of the M4U at the E-ELT is planned in 2024, after the electromechanical and optical calibration scheduled in 2022 in Europe. We will describe hereafter the test concept for the optical calibration of the M4U, as it is now at the middle of the final design phase.

1.1 The Optical Test Tower (OTT)

The optical calibration of the M4U will be performed via interferometry on a dedicated Optical Test Tower (OTT). The optical design is based on a beam expander setup[2] to generate a 1.5 m collimated beam to test the M4U at normal incidence. The test beam is smaller than the aperture of the M4U, but sufficient to image the single segment shell. The test configuration, reported in Fig. 1, is composed by a parabolic collimator and a relay system to shift the focal point outside the tower and limit the beam vignetting. The converging beam from the interferometer is folded downwards after the relay system by the folding mirror (FM), and collimated by the parabolic mirror[3] (PAR). The beam impinges M4 normally, and is reflected back along the same optical path. The proposed configuration is the best in terms of performances, manufacturing capabilities and costs

Further author information:
Runa Briguglio: E-mail: runa@arcetri.astro.it, Telephone: +39 055 2752200

Adaptive Optics Systems V, edited by Enrico Marchetti, Laird M. Close, Jean-Pierre Véran, Proc. of SPIE Vol. 9909, 99097A
 · doi: 10.1117/12.2231634

obtained at the end of the trade-off study of different solutions performed during the preliminary design phase. The possibility of testing the entire M4U aperture with a single 2.4 m collimator was discarded because of ESO requirements concerning the overall OTT volume. The test setup will include also a $\approx$ 0.5 m diameter perfectly flat mirror as reference (RF), to be inserted in the interferometric cavity for alignment verification purposes. Thanks to the collimated test beam, it is possible to look either on the RM or on the M4 shell without modifications of the test setup. The OTT will also allow a rotation of the test beam around the M4 axis and its translation in a plane normal to M4. These movements are required to complete the whole set of measurements necessary to collect the entire mirror shape.

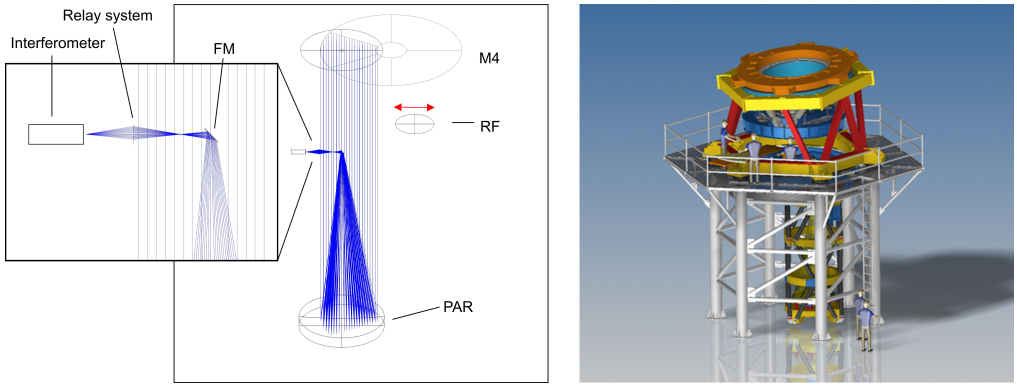

Figure 1. Scheme of the Optical Test Tower (left) and layout of the mechanical design (right).

1.2 Test concept

The idea to limit the beam aperture while maintaining the concept of a full aperture test comes from the requirement to reduce the OTT volume; additionally, a better sampling of the M4U surface is obtained in terms of high orders (HO). This approach leads us to the concept of the macro-stitching.
In facts, the test beam in the OTT allows the calibration of the single shell, that can be seen as a sub-aperture of the whole mirror. After the separate calibration and flattening of the six mirror segments, the petals co-phasing is necessary to provide the mirror the surface continuity. The test plan at the single shell level is derived from our experience with the LBT[4] and DSM calibrations,[5] but then peculiarities arise for the segmented nature of the mirror.

1.2.1 Flattening at the single shell

After the preliminary flattening, consisting in the identification of a set of actuator commands to have the whole mirror surface within the interferometer capture range, it is possible to collect the set of mirror modes (modal and zonal influence functions) required to complete the flattening procedure and the correction of the high order modes. Low order modes, like piston and tip-tilt, are not corrected at this point. A great attention shall be paid at this stage to avoid correcting the alignment HO like coma and spherical aberration with the M4U surface. The calibration[6] of the capacitive sensors, co-located with the single actuators, is also performed with a procedure run separately for each shell. At this step, the presence of neighbor non-active shells may be used for the correction of vibration noise on the measurement area.

1.2.2 Phasing of the shells

In order to co-phase all the segments, differential tip/tilt and piston is corrected with the following procedure:

1. the OTT is configured as to image the central part of the M4U;
2. local tip/tilt is removed;
3. the differential piston is measured with a dedicated Piston Sensing Unit[7] (PSU) . This is necessary to remove the lambda ambiguity of the interferometric measurements;

4. the final phasing is completed with the interferometer, with a goal phasing accuracy of 20 nm RMS wavefront.

1.2.3 Zernike modes test

The open loop calibration of the flattening command for the non-adaptive operation of the telescope is also requested, along with the measurement of the Zernike fitting error upon the open loop application of 10 μm WF Zernike command (for the first 11 modes only, computed over the M4 optical area).

1.2.4 Requirement verification

The OTT has been designed to certify the M4U at different spatial scales, depending on telescope constraints. M4U shall deliver the following performances:

- the surface error shall be less than 1.0 arcsec RMS slope, with a limited force budget;
- the wavefront at the 30 mm spatial scale smaller than 20 nm RMS (residual high order aberrations)
- the wavefront at the 60 mm scale smaller than 1 μm PtV along the edges of the M4 Mirror Shells, to reduce errors at the shell gap;
- the local curvature radius larger than 20 km on spatial scales of 80 mm or larger, which derives from the scalloping of the segmented primary mirror.

1.3 Lesson learned from the optical test of the M4DP

The M4U Demonstration prototype (M4DP) is a technical demonstrator of the final unit and is composed by two trapezoidal segments, sized $\approx$ 30cm x70cm, controlled by 111 actuators each. The control electronics and communication interface are the replica of those of the M4U. The M4DP was subjected to optical calibration[8] as a part of Preliminary Design Review of the M4U project: the tests allowed us to start defining the M4U calibration strategy and to address in advance some related potential issues. Here we will give a short recall of the lesson learned.

We managed such segmented system as whole, by assembling the individual configuration matrices (such as the *Feed Forward* or the eigenmmodes matrices) as block-diagonal; in such a way, all the commands were contemporary applied on both subsystems. When collecting the optical interaction matrices, we used the *a priori* information that one shell was not acted to measure the local tip-tilt from vibration and correct it on the acted shell; then the low order modes were effectively decoupled from vibration noise. This allowed to include the segment tip-tilt in the interaction matrix as a combination of mirror modes in order to compensate for the differential tilt between the segments with a suitable actuator command. The measurement and correction of the segment piston was also attempted and we successfully tested an algorithm for the compensation of the interferometer phase ambiguity. The Zernike modes test was also performed and we defined a procedure for the close loop application of the Zernike shapes: the procedure consists in applying an open loop pure piston command, equal to the wanted Zernike mean value over the shell area, then the flattening procedure is run considering the theorical Zernike shape as the goal. The procedure resulted in an accuracy in the application of the Zernike command comparable to that of the flattening ($\approx$ 20 nm RMS WF).

2. OPTICAL CALIBRATION OF THE M4: OPEN POINTS

Despite the results achieved on the M4DP, many questions remained un-answered. The M4DP was indeed just partially representative of the final system, both in terms of optical set-up and measurement strategy: in particular some of the DP test cases were addressed following a problem-oriented approach (triggered by the specific set-up), so that a generalized response is still missing.
In this section we will summarize these open points.

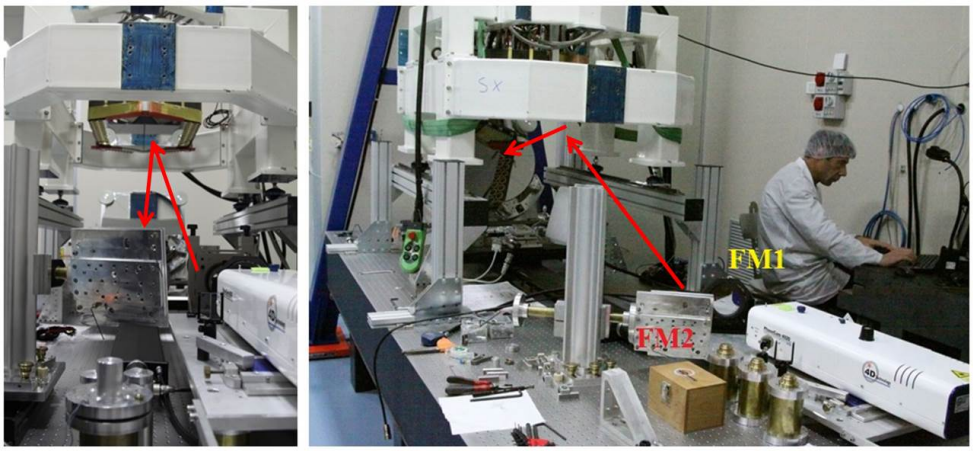

Figure 2. Optical bench for the measurement of the M4DP.

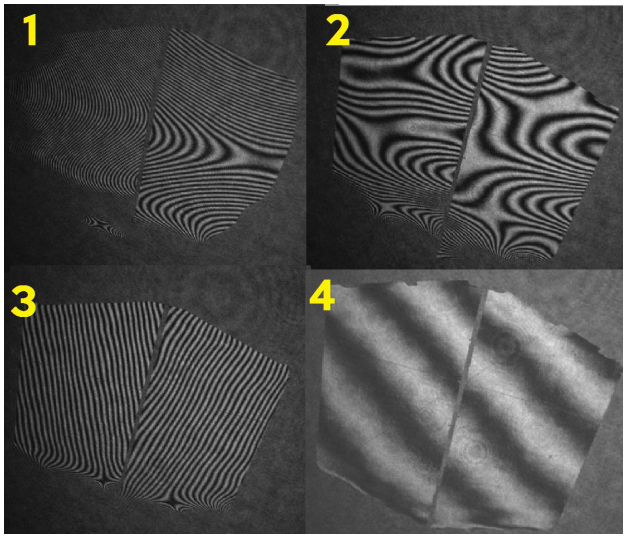

Figure 3. The 4-steps flattening procedure as performed on the M4DP: the first alignment; preliminary flattening; high orders flattening; the co-phasing.

2.1 Phase ambiguity and islands piston

The interferometer SW transforms the fringes images captured by the CCD into phase maps. The fringes are a periodic signal, so that the interferometer is not sensitive to the absolute distance of the test surface and the SW will assign an offset to the phase maps. Such offset is not fully arbitrary, as it is constrained by the fringes intensity: it follows that the offset shall be an integer of the interferometer wavelength, $n\lambda$. We can outline such procedure, for simplicity, with the SW taking the first valid pixel in the frame, computing the corresponding phase lag from pixel fringe intensity and offsetting the result by $n\lambda$; the following pixels will be referenced with the previous one. According to this plot, the pixel-to-pixel difference between two phase maps of a rigid surface is a plane at $(n_1 - n_2)\lambda$. Three consequences comes from such statement.

First, the piston value of a given surface measured on the frame is affected by $n\lambda$ ambiguity. Such issue is of minor importance as we may discard the mirror "true" piston.
On the opposite (second point) when comparing two or more phase maps, we need to solve such $differential$ phase ambiguity, in order to restore for each frame the initial $n_0\lambda$ uncertainty.
Things get more complicated (third point) when the measured surface is divided into islands, which are areas on the fringes frame separated by more than 2, 3 pixels (enough pixels to prevent the interferometer SW to run

any interpolation routine to reconnect them). Islands phase maps are observed, for instance, on a segmented mirror or on a monolithic surface where the shadow of a spider arms divides the frames into patches. In islands phase maps, the $n\lambda$ ambiguity applies for each of the islands, each with a different n_i. Such effect may be easily recognized if we consider, according to the schematization given above, that each island has its own *first pixel* to start the phase unwrapping process with. All these three issues have been observed during the optical test of the M4DP. So far, *phase ambiguity* is an additive offset for each frame: associative property applies so that the sum/difference of frames is still degenerate by $(n_i \pm n_j)\lambda$; again, because of distributive property, the distribution of the averaging of m frames is scattered with $n/m\lambda$ spread. According to these statements, it is possible to sketch a procedure to reconnect at the same (initial, e.g.) phase a sequence of frames or an ensemble of islands in the same frame; because phase ambiguity is an intrinsic limitation of the interferometer as a phase sensor, some *a priori* assumptions should be considered: for instance, that the frame-to-frame "true" jumps (e.g. vibration) shall be lower than λ. Under this condition, a piston-unwrapping algorithm is feasible and has been implemented and successfully tested during the M4DP optical verification. We noticed that the validity of the condition is not guaranteed in presence of large environment vibration and convection noise.

2.2 Measurement of the mirror piston signal

The concept of *piston-unwrapping* may be extended to the case of measuring the piston response of an actuator command. We are now considering a push-pull measurement, i.e. the difference between two phase maps ϕ_1 and ϕ_2 measured after applying two opposite actuator commands $c, -c$. The wanted piston response p_c may be calculated as in the following

$$\phi_1 = \phi_{HO} + p_c + \epsilon_1 + n_1\lambda \quad (1)$$

$$\phi_2 = -\phi_{HO} - p_c + \epsilon_2 + n_2\lambda \quad (2)$$

$$< \phi_2 - \phi_1 > = 2p_c + \epsilon + (n_2 - n_1)\lambda \quad (3)$$

where we put $\phi_{HO} :< \phi_{HO} >= 0$ is the high order components and $\epsilon :< \epsilon >\neq 0$ is the measurement noise from vibration and air convection. The measurement may be piston-unwrapped as described in Sec.2.1 provided that $2p_c + \epsilon < \lambda$.

For a DM like the M4 or the M4DP, the optical piston is generated with a linear combination of the first low order stiffness modes; because of the initial mis-calibration of the capacitive sensors, it is not possible to know the mode amplitudes *a priori* and a direct measurement is required. It follows that the interaction matrix of the first low order modes should be collected with a pretty low amplitude, in order to not saturate the $\lambda/2$ threshold. Such condition is rather unfavourable, as one wants to measure them with very good SNR to maximize the flattening precision. Also, low order modes fit well the tip-tilt shapes, so that low order influence functions are not re-aligned after measurement (while high orders are) to preserve the ability to correct individual segment tilt. Because of cross-talk with vibration noise, again low order modes need to be measured with very large amplitude.

A possible strategy could be to create an arbitrary command matrix where the first mode has a large component of optical piston, while the others provide a negligible contribution to it. Then, just the first mode needs to be measured with low command amplitude and one may improve the SNR by increasing the time integration on that peculiar mode only.

2.3 Local measurement, global correction

In OTT the diameter of the test beam is 1.5 m, so that the entire M4 doesn't fit a single interferometer frame. There are two possible configurations of the test tower: with the test beam measuring a single segment, at the center of the frame, or with the test beam illuminating the central portion of the M4, with all the segments partially visible.

In order to attain the flattening command of all the segments, separately, the first configuration is valid. On the contrary, when one wants to correct the individual segment tip/tilt to co-phase the entire mirror surface, such configuration requires the movement of the rotating assembly in OTT to align each segment with the previously measured one. Such procedure has the drawback to introduce a significant amount of alignment tilt when rotating the tower, so that co-phasing is seriously affected. A backup strategy is to aim at the central part

of M4 and correct the segment tip-tilt based on the optical measurement of that part only. The point here is the control of unseen actuators, as the large outer area of all the segments is beyond the frame size. A strategy to be investigated is to constrain the command on the unseen actuators by imposing a geometrical condition (i.e. pure tip-tilt) on the shape applied.

2.4 Images management

Within OTT we expect four issues related to images management.

ROI masks Detector masks will be divided into ROI (regions of interest) corresponding to the 6 M4 segments. The ROI recognition and proper indexing (despite OTT rotation and displacement) is of capital importance to allow the automation of the optical calibration process.

Optical cavity subtraction Given the very tight WFE specification on the flattened M4, we are requested to measure and subtract the PM surface map. The correction is effective as long as the PM map is properly aligned and geometrically transformed to match the current PM orientation within the test beam. We budgeted 2 pixel as the maximum allowed alignment error to match the specification for M4.

IF remapping In order to allow an older set of Influence functions to flat the mirror, the corresponding interaction matrix must be re-aligned to match the current OTT geometry. To this purpose, some marker (a few actuator IF, e.g.) shall be added to any measurement to allow the alignment at a later time.

Segment images composition The final image of the entire M4 mirror surface will be composed by (at least) 6 separated frames, each captured with its peculiar alignment residuals. The footprint of the cavity will be also replicated in each frame. An image macro-stitching algorithm should then be prepared to allow the frames composition while rejecting the differential alignment and the constant cavity surface error.

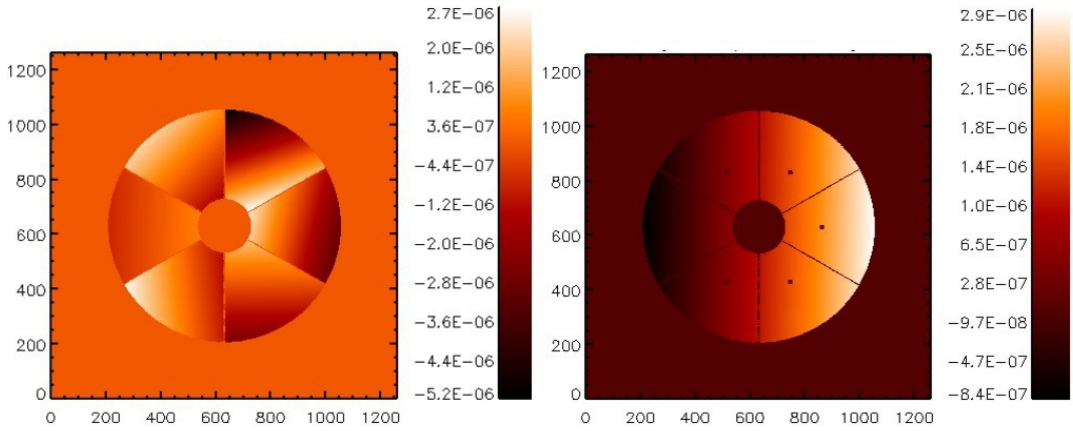

Figure 4. Example of the macro-stitching concept, where the individual segment measurements (flat in the present case for simplicity) are digitally aligned to provide a final M4 surface measurement.

2.5 OTT alignment

We need to cope with two main issues concerning the OTT alignment: tight wavefront error budget and aberration crosstalk with the M4 shape. The first point is the very tiny margin for the measurement of the wavefront coming from optical alignment residuals: the need is to measure such residuals with an absolute accuracy of a few nm RMS over the M4 mirror segment area. We recall here that the optical alignment is performed with a ≈ 50 cm diameter flat mirror to provide a reference surface. As the flat mirror is smaller than the beam, we expect that accuracy errors may come from partial sampling of the aberrated wavefront; the position of the mirror within the beam may also contribute to this effect.

As a second point, Zernike modes as coma, defocus and spherical aberration are indistinctly produced by misalignment of the optical elements and by the deformable mirror. The alignment procedure should therefore preserve these shapes on the M4 while compensating the same aberration in the beam by proper positioning of the parabola. The flat reference mirror is of great help to this purpose, as the aberrations are measured on a rigid surface; however during the last step of the alignment, the mirror should be extracted from the cavity to have full visibility of the M4, so that the optical alignment at that stage should be performed without an absolute feedback.

3. 8S, THE OPTICAL TEST TOWER SIMULATOR

3.1 Concept and goal

The tool is a generator of the interferometer phase maps produced with M4 on the OTT under the given system configuration. Images are created and stored with the relevant environment and meta-data according to the data tree commonly adopted for the optical calibration of the LBT, VLT, M4DP deformable mirrors. Within this frame, two tasks are accomplished: first, the entire calibration procedure may be simulated simply by replacing the interferometer sampling command with the 8s frame generation; second, simulated data may be processed with the analysis tool we developed for optical calibration of DMs, for instance to check the test specifications. In general, the tool has been prepared in order to provide an answer to the open points outlined in Sec.2. With simulation we expect then to obtain the right set of OTT actions (sequence of alignment, configuration change, actuator commands, e.g.) and sampling parameters (command amplitude, integration time, e.g.) to produce a result within specifications. A secondary output of the tool is to provide an estimation of measurement noise to fill the test error budget table. In this section we will give a functional description of 8s.

3.2 Simulator architecture

3.2.1 Input data

The primitive dataset to create a simulated OTT phase map comes from the tower and mirror model and are described in the following.

OTT optical design model According to the optical prescription of the OTT, the sensitivity of each optical elements are computed, in terms of amplitude of the first 11 Zernike modes versus optics displacement (5 degrees of freedom).

M4 Finite Element model The M4 actuator Influence Functions are generated with the FE model of the mirror segment and replicated with a 60° symmetry to provide a full system description. The model includes also the effect of the lateral flexures holding the glass shells. In[9] an exhaustive comparison between FE and real data IF of voice coil DMs is given.

OTT FE and mechanical design The mechanical design of the OTT provides all the relevant sizes of both optical and mechanical elements. Given the interferometer resolution the image plate scale is automatically found. The OTT FE model has been also used to compute the elements displacement after rotation/translation of the moving assembly. The FE dataset has been provided by ADS-International who will responsible for the integration of the test tower.

Noise model Vibration noise has been modelled considering a typical vibration spectrum measured in a *quite* laboratory, then low-pass filtered according to the tower insulators specification, then propagated (through FEA) to the optical elements.

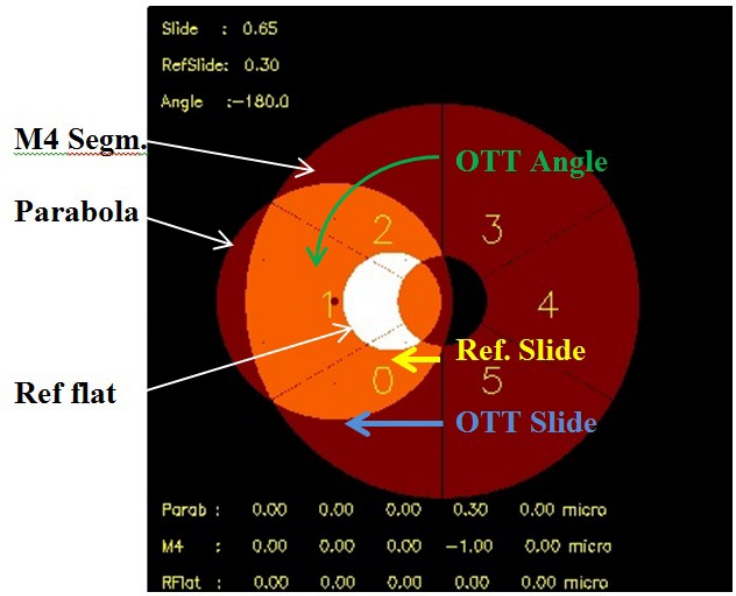

Figure 5. Description of the 8s inputs as OTT components.

3.2.2 Operator input

Modifying the system parameters (like applying actuator commands or reconfiguring the OTT geometry) is the building element of the optical calibration. To this scope, the user is allowed to modify the following system parameters.

- *OTTslide* in order to capture a single segment or the M4 mirror center. The parameter may accept any value, to test for instance different segment geometry within the frame.
- *OTTangle* to rotate the parabola holder and aim at different segments.
- Optical elements position, in terms of rigid body motion provided by alignment stages (e.g hexapod)
- Actuator commands.
- Interferometer time average, in terms of number of frames to be averaged together to reduce the vibration noise.
- Vibration noise on/off, interferometer phase ambiguity on/off, cavity offset (polishing residuals) on/off.

3.2.3 Image creation

The core of 8s is the generation of simulated OPD by the interferometer, corresponding to the phase maps of M4 as measured with the current configuration of the OTT. The procedure for the phase map generation is as follows.

1. an empty interferometer frame Q of nx, ny pixel is generated; a circular mask M is drawn as the parabola footprint and the parabola polishing residual is added; the image resolution is given by the parabola radius and the frame size;
2. the shape of M4 corresponding to the current actuator command is generated; both the full M4 image and mask (with segment ROIs) are cropped and rotated according to the current OTT geometry;
3. the reference flat mirror mask and (flat) shape are generated and positioned in Q according to its current configuration;

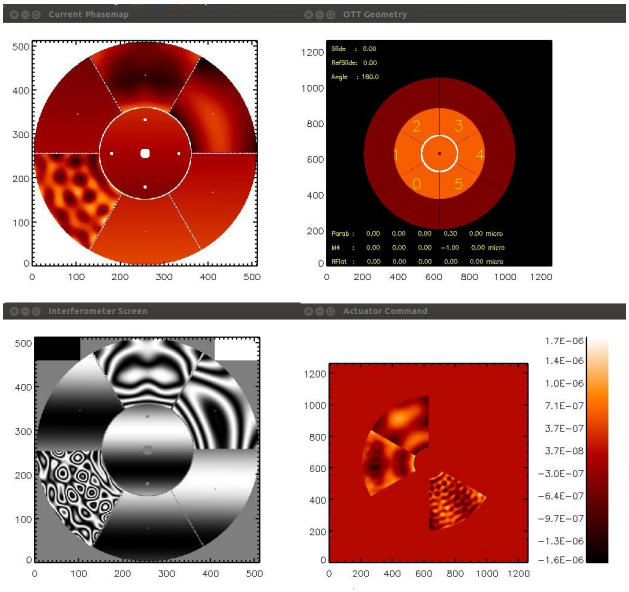

Figure 6. OTT phasemaps simulated with 8s, at the in-center configuration, whit the parabolic mirror looking at the central part of all the segments. Tip/tilt from vibration is added.

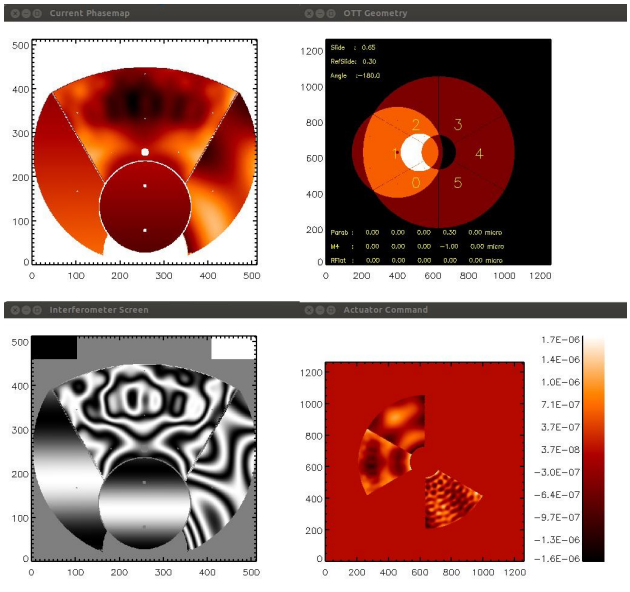

Figure 7. Ott phasemap with the parabola viewing at segment 1.

4. if noise is enabled, the 5 elements position vector of each optics is perturbated according to the time evolution at the current time of the considered vibration spectrum; the alignment aberration for each optical elements are computed from their actual position and added to their current images;
5. the Q frame is updated by adding all the optics images and masked accordingly;
6. if enabled, the individual ROIs within M are found and a random integer λ offset is added to each. The final Q frame is displayed and the relevant OTT configuration data are logged.

3.3 Verification and preliminary results

The simulator has been verified by cross-checking its outputs with the wavefront map obtained by an optical design software. After verification, we started building up the M4 test plan, writing down the procedures and simulating them. In the following we will report a preliminary resume of the work completed so far.
For the OTT alignment (see Sec.2.5) we computed a *mixed* interaction matrix of the parabola and the reference flat together and nulled the alignment Zernikes over the mirror pupil; M4 was aligned by nulling tip/tilt only: this procedure removes automatically the alignment coma which is entangled with tip/tilt, leaving unchanged the coma from M4 surface shape C_{M4}. After extracting the reference, the residual alignment was corrected by moving together the parabola and M4: we considered the shape C_{M4} as an offset for the alignment command computation, thus preserving once more the figuring aberrations, to be corrected with an actuator command. We also investigated the effect of partial spatial sampling of the alignemnt Zernike modes as measured on the small reference flat. We estimated the accuracy of the Zernike fitting on the flat while changing its position within the beam and changing its diameter. The results are given in Fig.9, showing that the accuracy in the estimation of coma and focus is better than 0.2% for any mirror position within the beam.
The single segment flattening was simulated according the procedure developed for the LBT and VLT; we included also the measurement of the actuators influence functions (some are presented in Fig.8) with tip/tilt correction as experimented with the M4DP (refer to Sec.1.3), allowing the flattening of the segment tip/tilt. The multiple segments phasing has been also addressed, although limited so far to differential tip/tilt correction. The result of the individual segment flattening is given in Fig.11: there, the segments are also correctly co-phased because no differential piston was added so far in the simulation.

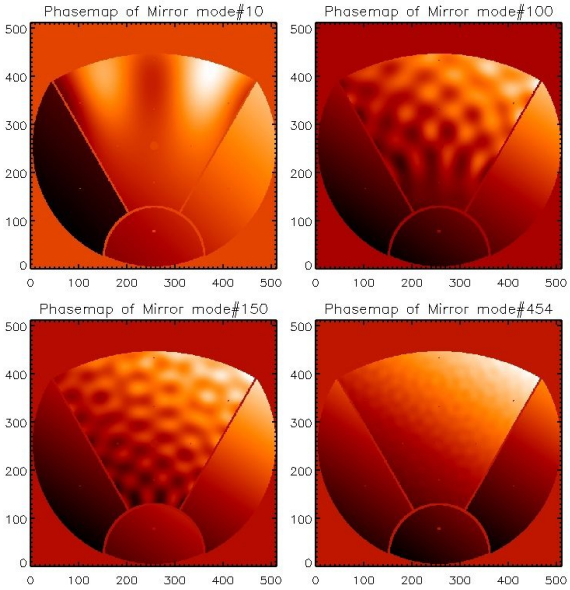

Figure 8. A sample of mirror modes measured on segment 1, including the differential piston from interferometer phase ambiguity.

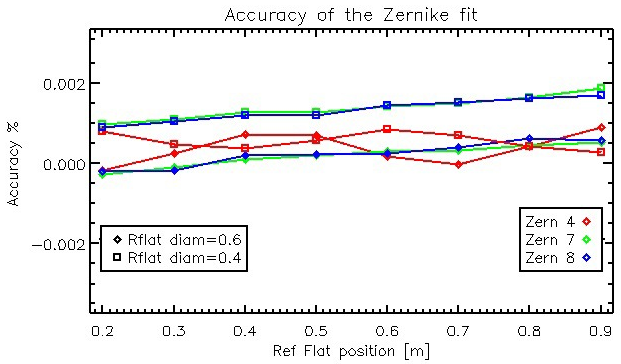

Figure 9. Accuracy error for the Zernike fit of the alignment modes as measured on the reference flat, smaller than the optical pupil.

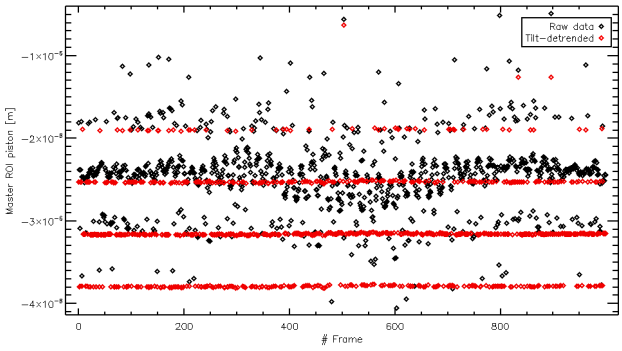

Figure 10. Test of differential piston measurement with noise, after phase ambiguity solution and vibration noise correction.

4. CONCLUSION

M4, the wavefront corrector of the E-ELT, will be the largest deformable mirror equipping an astronomical AO system. The optical calibration will be performed on a test tower called OTT, where the single segment flattening and the global phasing will be performed to provide the DM with the calibrations needed for the AO loop. We experienced the optical test on a segmented mirror with the M4 demonstration prototype and identified the development path.

We set-up a numerical simulator of both the M4 and the OTT, a tool to help building up the test plan and procedures and address the criticalities in the optical test. So far, we simulated the OTT alignment and single segment flattening and identified the procedures for measuring the piston signal produced by the mirror modes. The optical test of M4 is scheduled to start in 2022.

REFERENCES

[1] Vernet, E., Cayrel, M., Hubin, N., Mueller, M., Biasi, R., Gallieni, D., and Tintori, M., "Specifications and design of the E-ELT M4 adaptive unit," in [*Adaptive Optics Systems III*], *Proc. of SPIE* **8447**, 844761 (July 2012).

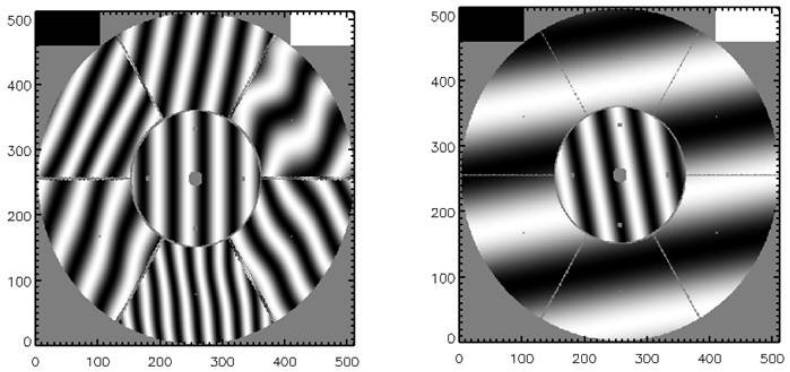

Figure 11. Test of segments phasing with the correction of the differential tip/tilt.

[2] Pariani, G., Briguglio, R., Xompero, M., Riccardi, A., Riva, M., Bianco, A., Zerbi, F. M., Tresoldi, D., Molinari, E., Tintori, M., Lazzarini, P., Gallieni, D., Biasi, R., Vernet, E., and Cayrel, M., "Approaches to the interferometric test of large flat mirrors: the case of the adaptive M4 for E-ELT," in [*Ground-based and Airborne Telescopes V*], *Proc. of SPIE* **9145**, 91453B (July 2014).

[3] Pariani, G., Tresoldi, D., Moschetti, M., Riva, M., Bianco, A., and Zerbi, F. M., "Metrology of flat mirrors with a computer generated hologram," in [*Advances in Optical and Mechanical Technologies for Telescopes and Instrumentation*], *Proc. of SPIE* **9151**, 91510Y (July 2014).

[4] Riccardi, A., Xompero, M., Briguglio, R., Quirós-Pacheco, F., Busoni, L., Fini, L., Puglisi, A., Esposito, S., Arcidiacono, C., Pinna, E., Ranfagni, P., Salinari, P., Brusa, G., Demers, R., Biasi, R., and Gallieni, D., "The adaptive secondary mirror for the Large Binocular Telescope: optical acceptance test and preliminary on-sky commissioning results," in [*Adaptive Optics Systems II*], *Proc. of SPIE* **7736**, 77362C (July 2010).

[5] Briguglio, R., Xompero, M., Riccardi, A., Andrighettoni, M., Pescoller, D., Biasi, R., Gallieni, D., Vernet, E., Kolb, J., Arsenault, R., and Madec, P.-Y., "Optical calibration and test of the VLT Deformable Secondary Mirror," in [*Proceedings of the Third AO4ELT Conference*], Esposito, S. and Fini, L., eds., 105 (Dec. 2013).

[6] Briguglio, R., Xompero, M., Riccardi, A., Biasi, R., and Andrighettoni, M., "Optical calibration of capacitive sensors for AO: strategy and preliminary results," in [*Adaptive Optics Systems III*], *Proc. of SPIE* **8447**, 84474E (July 2012).

[7] Molinari, E., Tresoldi, D., Toso, G., Spanò, P., Mazzoleni, R., Riva, M., Riccardi, A., Biasi, R., Andrighettoni, M., Angherer, G., Gallieni, D., Tintori, M., and Marque, G., "The optical tests for the E-ELT adaptive mirror demonstration prototype," in [*Adaptive Optics Systems II*], *Proc. of SPIE* **7736**, 773632 (July 2010).

[8] Briguglio, R., Xompero, M., Riccardi, A., and al., "Optical calibration of the M4 prototype toward the final unit," in [*Proceedings of the Fourth AO4ELT Conference*], (2015).

[9] Del Vecchio, C., Briguglio, R., Riccardi, A., and Xompero, M., "Analysis of the static deformation matching between numerical and experimental data on the voice-coil actuated deformable mirrors," in [*Adaptive Optics Systems IV*], *Proc. of SPIE* **9148**, 914840 (Aug. 2014).